PRAMANA
— journal of
physics

Vol. 68, No. 5
May 2007
pp. 831–842

Computation of surface roughness using optical correlation

A M HAMED[1] and M SAUDY
Department of Physics, Faculty of Science, Ain Shams University, Cairo, Egypt
[1]Present address: Department of Physics, Faculty of Education at Sur, P.O. Box 484, Postal Code 411, Sultanate of Oman
E-mail: amhamed73@hotmail.com

MS received 1 March 2006; revised 5 October 2006; accepted 5 January 2007

Abstract. The laser speckle photography is used to calculate the average surface roughness from the autocorrelation function of the aluminum diffuse objects. The computed results of surface roughness obtained from the profile shapes of the autocorrelation function of the diffuser show good agreement with the results obtained by the stylus profile meter.

Keywords. Surface roughness; optical correlation; speckle.

PACS Nos 68.47.De; 42.30.Ms; 78.68+m

1. Introduction

It is known that the surface profiles [1–4] are classified as: (i) Amplitude parameter which measures the vertical heights of the surface deviations from a reference line. (ii) Spacing parameter that measures the horizontal characteristics of the surface deviations. (iii) Hybrid parameter which is a combination of both amplitude and spacing parameters.

These parameters are the basic factors that affect the surface profile and the first parameter (amplitude) is defined as the surface roughness. We assume that the height profile of a given surface is a single valued function of the point coordinate $h(x)$. There are two measures of surface roughness:

(i) the average height of the profile R_a which is given as

$$R_\mathrm{a} = \langle h \rangle = \frac{1}{L}\int_0^L |h(x)|\,\mathrm{d}x,$$

where L is the transverse measured length.

The other measuring parameter is the root mean square (rms) surface roughness and it is defined as

$$\sigma = R_{\mathrm{rms}} = \sqrt{\int_0^L Y^2\,(x)\,\mathrm{d}x},$$

where $Y(x) = h(x) - \langle h \rangle$ is the deviation from the mean surface roughness. The rms surface roughness describes the fluctuations of surface heights around an average surface height. The above equations represent zero-order statistics while the surface height distribution function $p(x)$ is considered as the first-order statistics. The latter function gives the probability of the emergence of height (h) at a given point of the surface. It is positive and normalized such that

$$\sum_i p_i(h) = 1.$$

When the detailed height profile is unknown, the Gaussian height distribution may be suitable to represent the surface roughness as follows:

$$p(h) = \frac{1}{\sqrt{2\pi\sigma}} \exp\left(-\frac{h^2}{2\sigma^2}\right).$$

The mechanical stylus profile meter [5–8] is used to measure accurately the mean surface roughness of rough objects within one micron. It is common to cite that resolution measurements of surface roughness parameter depend on the diameter of the measuring needle tip of the apparatus. Also, mechanical stability of the apparatus is required for the measurements to be within the range of measurement. Unfortunately, this apparatus can damage the surface under investigation. Moreover, the measured profile is a convolution of the true surface profile and the stylus radius [7]. So, optical interference and light scattering techniques are recommended to measure the mean surface roughness with a great accuracy without damaging the surface. By these methods, surface roughness can be measured within a small fraction of the wavelength of light used [8].

Different optical techniques were used to measure surface roughness. The light-scattering technique for surface roughness measurements has received wide attention in the past few decades [9–15]. The theoretical background of this technique is based on Beckmann's rough-surface scattering model [16,17]. Also the autocorrelation function of the surface height variations is determined from the scattered intensity. Basically, this technique is applied to moderately rough surfaces, usually with heights less than 4 μm.

The Fourier spectrum analysis technique [18–22] assesses surface roughness by analyzing the distribution of the spatial frequency of the scattered light. The upper limit for the measurement of roughness with the Fourier technique is less than 2 μm, although a roughness up to 5 μm has been successfully measured [21].

The speckle-contrast technique relates object surface roughness to the contrast of the speckle image, which is a scale of the speckle-intensity variation [23–26]. This relationship is obtained from the statistical properties of speckle images [23]. In practice, translation of either the test surface or the photo-detector is necessary to detect a sufficient intensity of the speckle field for the calculation of the average contrast of the speckles. This technique is subsequently extended to the use of a charge coupling digitization (CCD) camera to record the whole speckle image and to achieve a real-time measurement of ground surfaces [27]. However, the roughness measuring range with the real time technique is limited to be within a fine range less than 0.3 μm.

In the speckle-correlation technique [28], a double-exposure speckle photography technique is used. The laser source has to be rotated between exposures and two speckle patterns are recorded on the same photographic film. There is a strong relation between the object surface roughness and the degree of correlation of the two speckle patterns. Information on surface roughness is derived from the obtained contrast of the resulting fringe pattern in the Fourier plane. This method is subsequently extended to real-time measurement through the use of two Michelson interferometers [29] and a CCD camera, which records the formed Young's fringes [30]. Recently, Hamed *et al* [31] published an assessment of surface roughness from the speckle binary images based on signal-to-noise ratio. Recent research on the surface roughness measurement has been developed based on laser scattering technique for more speedy surface inspection [32–35].

In this paper, a quantitatively simple method, based on optical correlation, is used to determine the average surface roughness compared to that based on interference investigated by Leger *et al* [28]. They have obtained the surface roughness from the contrast measurements of the resulting fringe pattern in the Fourier plane. The former method is based on the detection of the autocorrelation intensity of the diffuser function in order to compute the average surface roughness. The theoretical analysis is followed by experimental measurements and finally a conclusion is given.

2. Theoretical analysis

An inclined plane wave emitted from laser beam is incident, at an angle θ, on the normal to the rough object $g(x,y)$ as shown in figure 1. The reflected wave passes through a Fourier transform lens of focal length f and is measured by a light detector as a function of local spatial coordinates (ξ,η). The laser beam may have cross-section with area $A=\pi D^2/4$ of diameter D and constant power density ρ_{p}. The reflectance of the rough surface $R=|r|^2$. Then, we have the incident inclined plane wave as

$$E_i(r,t)=E_0\exp[i(kz-\omega t)]\exp[-iky\sin\theta], \tag{1}$$

where $\omega=2\pi c/\lambda$ is the angular frequency of light and $k=2\pi/\lambda$ is the wave vector. At the rough surface, the inclined plane wave becomes modulated with respect to its phase and so the amplitude of the wave reflected directly at the surface (near field) is given by

$$E_N(x,y,z=0)=E_0 r\exp[-ik2g(x,y)]\exp[-iky\sin\theta]. \tag{2}$$

Then the far field in the focal plane of the Fourier transform lens as a function of local variables (ξ, η) is obtained by operating the FT upon eq. (2) as follows:

$$E_{\mathrm{F}}(\xi,\eta)=\frac{1}{A}\int\int_A E_N(x,y,z=0)\mathrm{e}^{-i\frac{2\pi}{\lambda f}(x\xi+y\eta)}\,\mathrm{d}x\,\mathrm{d}y. \tag{3}$$

Substitute eq. (2) in eq. (3), then we get

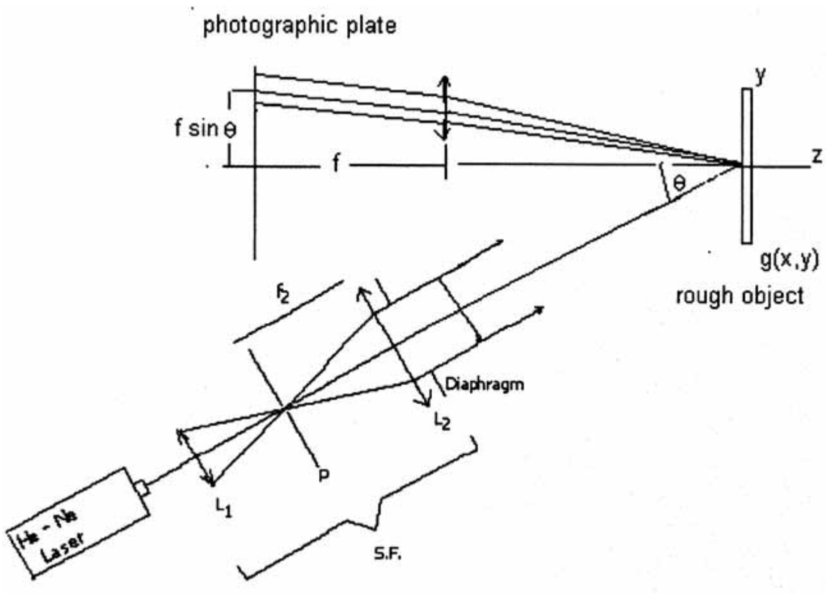

Figure 1. Optical arrangement used for recording speckle patterns. SF: spatial filter; L_1: an objective lens of short focus; P: a pinhole; L_2: lens of focal length $f_2 = 15$ cm; g: rough object situated in the plane (x, y). The wavelength of the illumination $\lambda = 0.6328$ μm; $D = 1$ cm is the cross-section of the beam covering the surface. The photographic film is placed in the plane (η, ζ) which is the focal plane of the Fourier transform lens of focal length f.

$$E_{\mathrm{F}}(\xi,\eta) = \frac{E_0 r}{A} \int\int_A \exp[-ik2g(x,y)] \times \exp[-iky\sin\theta]\, \mathrm{e}^{-i\frac{2\pi}{\lambda f}(x\xi+y\eta)}\, \mathrm{d}x\, \mathrm{d}y. \tag{4}$$

Making use of convolution operations [36], the Fourier transformation in eq. (4) can be written in abstract form as follows:

$$\begin{aligned} E_{\mathrm{F}}(\xi,\eta - f\sin\theta) &= \frac{E_0 r}{A}\,\mathrm{FT}\{\exp[-ik2g(x,y)]\} \otimes \mathrm{FT}\{\exp[-iky\sin\theta]\} \\ &= \frac{E_0 r}{A}\,\mathrm{FT}\{\exp[-ik2g(x,y)]\} \otimes \delta(\xi,\eta - f\sin\theta). \end{aligned} \tag{5}$$

The intensity located in the plane (ξ, η) is the modulus square of the far field diffraction and is represented as follows:

$$I_s(\xi,\eta - f\sin\theta) = |E_{\mathrm{F}}(\xi,\eta - f\sin\theta)|^2. \tag{6}$$

The expectation value of the recorded intensity is given by

$$\langle I_s(\xi,\eta - f\sin\theta)\rangle = \langle E_{\mathrm{F}}(\xi,\eta - f\sin\theta) E^*_{\mathrm{F}}(\xi,\eta - f\sin\theta)\rangle, \tag{7}$$

where $E^*_{\mathrm{F}}(\xi,\eta - f\sin\theta)$ is the complex conjugate of the complex amplitude of the speckle pattern centered at $\xi = 0, \eta = f\sin\theta$. This is an exact analysis valid for any rough object without any approximation when compared with the case where $2k_Z\|g\|_\infty \ll 1$, and taking in to consideration the angle of incidence (θ) of the inclined plane wave and $\|g\|_\infty$ denotes the maximum norm.

In the former case of exact analysis, where $\|g\|_\infty \geq \lambda/4\pi$ we write eq. (7) as follows:

$$\langle I_s(\xi, \eta - f\sin\theta)\rangle = \frac{E_0^2 R}{A^2} \iint\limits_A \iint\limits_A \langle \mathrm{e}^{-ik2g(x,y)} \mathrm{e}^{+ik2g(x',y')}\rangle \times \mathrm{e}^{-\frac{2\pi i}{\lambda f}[\xi(x-x')+(\eta - f\sin\theta)(y-y')]}\, \mathrm{d}x\,\mathrm{d}y\,\mathrm{d}x'\,\mathrm{d}y', \qquad (8)$$

where $R = |r|^2$ is the reflected intensity from the rough object. Assuming the growth process of the surface height profile $g(x, y)$ to be translation invariant, the ensemble average autocorrelation function $\langle\ \rangle$ does not depend on absolute values of its variables, but only on the differences $x - x' = x''$ and $y - y' = y''$. By introducing these new variables we get

$$\langle I_s(\xi, \eta - f\sin\theta)\rangle = \frac{E_0^2 R}{A^2} \iint\limits_A \iint\limits_A \langle \mathrm{e}^{-ik2g(x,y)} \mathrm{e}^{+ik2g(x-x'',y-y'')}\rangle \times \mathrm{e}^{\left\{-\frac{2\pi i}{\lambda f}[\xi x''+(\eta - f\sin\theta)y'']\right\}}\, \mathrm{d}x\,\mathrm{d}y\,\mathrm{d}x''\,\mathrm{d}y'' \qquad (9)$$

for any arbitrary value of x, y. Interchanging with respect to (x, y) results in

$$\langle I_s(\xi, \eta - f\sin\theta)\rangle = \alpha \iint_A \langle \mathrm{e}^{-ik2g(x,y)}\ \mathrm{e}^{+ik2g(x-x'',y-y'')}\rangle \times \mathrm{e}^{\left\{-\frac{2\pi i}{\lambda f}[\xi x''+(\eta - f\sin\theta)y'']\right\}} \mathrm{d}x''\,\mathrm{d}y'', \qquad (10)$$

where $\alpha = E_0^2 R/2AZ_\omega$ is a constant value representing the maximum intensity of the reflected beam.

$$\begin{aligned}\langle I_s(\xi, \eta - f\sin\theta)\rangle &= \alpha \mathrm{FT}\ [\langle \mathrm{e}^{-ik2g(x,y)} \mathrm{e}^{+ik2g(x-x'',y-y'')}\rangle] \\ &= \alpha\,\mathrm{FT} \iint_A \mathrm{e}^{-ik2g(x,y)} \mathrm{e}^{+ik2g(x-x'',y-y'')}\, \mathrm{d}x''\,\mathrm{d}y'' \\ &= \alpha\,\mathrm{FT}\,[c(x, y)], \qquad (11)\end{aligned}$$

where $c(x, y)$ represents the autocorrelation function of the phase object $\exp[-ik2g(x, y)]$ of roughness height shape $g(x, y)$. So, the ensemble average speckle intensity is the Fourier transform of the autocorrelation function of $\exp[-ik2g(x, y)]$ as compared with the autocorrelation function of $g(x, y)$ obtained with the approximation $2k_Z\|g\|_\infty \gg 1$.

Operating the inverse Fourier transform on both sides of eq. (11), we obtain this result:

$$c(x, y) = \frac{1}{\alpha} \int_{-\infty}^{+\infty} \int_{-\infty}^{+\infty} \langle I_s(\xi, \eta - f\sin\theta)\rangle\ \mathrm{e}^{\left\{+\frac{2\pi i}{\lambda f}[\xi x+(\eta - f\sin\theta)y]\right\}}\, \mathrm{d}\xi\,\mathrm{d}\eta. \qquad (12)$$

Finally, without the cited approximation, we can find information about surface roughness from the autocorrelation function of the function $\exp\{-ik2g(x,y)\}$ using eqs (11) and (12). Hence, at zero path length we find

$$c(0,0) = \frac{1}{\alpha}\int^{+\infty}\int_{-\infty}\langle I_s(\xi,\eta - f\sin\theta)\rangle\,\mathrm{d}\xi\,\mathrm{d}\eta. \tag{13}$$

Special cases

(i) For $2k_Z\|g\|_\infty \ll 1$, i.e. $\|g\|_\infty \ll \lambda/4\pi$, the approximate wave after its reflection from the surface profile $g(x,y)$ is proportional to

$$\exp\{-ik2g(x,y)\} \cong 1 - ik2g(x,y).$$

Using eq. (11) and the above approximation, then we get this result:

$$\begin{aligned}\langle I_s(\xi,\eta - f\sin\theta)\rangle &= \alpha\,\mathrm{FT}\iint_A [1 - ik2g(x,y)] \\ &\qquad \times[1 + ik2g(x - x'', y - y'')]\,\mathrm{d}x''\,\mathrm{d}y'' \\ &= \alpha\,\mathrm{FT}\,[c(x,y)].\end{aligned} \tag{14}$$

The autocorrelation function becomes the Fourier transform inverse of the average speckle intensity eq. (12), with a constant part representing the aperture spread function. In this case $c(x,y)$ is given by the autocorrelation function of the surface height profile, i.e.

$$c(x,y) = \langle g(x,y)g(x - x'', y - y'')\rangle. \tag{15}$$

The corresponding rms roughness is obtained using eqs (13) and (15).

(ii) For roughness greater than the wavelength, we are obliged to take the higher terms in the exponential, and then we get this result;

$$\begin{aligned}\langle I_s(\xi,\eta - f\sin\theta)\rangle &= \alpha_1\,\mathrm{FT}\,\langle g(x,y)g(x - x'', y - y'')\rangle \\ &\quad + \alpha_2\,\mathrm{FT}\,\langle g^2(x,y)g^2(x - x'', y - y'')\rangle \\ &= \alpha\,\mathrm{FT}\,[c(x,y)].\end{aligned} \tag{16}$$

In this case, the autocorrelation function which is the Fourier transform inverse of the ensemble average speckle intensity is given by

$$\begin{aligned}c(x,y) &= \langle g(x,y)g(x - x'', y - y'')\rangle \\ &\quad + \beta\langle g^2(x,y)g^2(x - x'', y - y'')\rangle\end{aligned} \tag{17}$$

where $\beta = \alpha_2/\alpha_1$. Again, the rms roughness is obtained using eqs (13), (16) and (17).

It is clear that the surface information of the diffuse object is related to the autocorrelation function of the defined surface as stated in eq. (15). As an example,

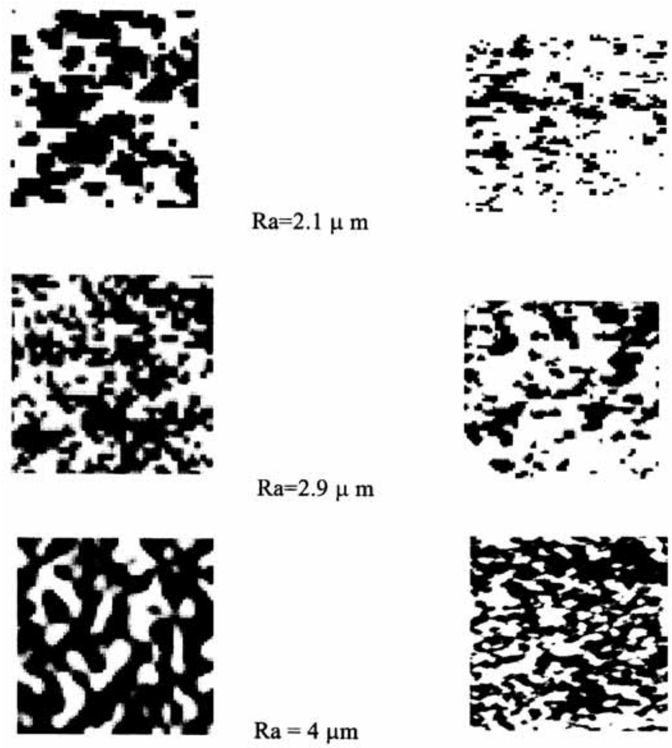

Figure 2. Detection of speckle images (left) and the corresponding autocorrelation images (right) for different surfaces of aluminum using CCD camera.

we take a simple rectangular function of width a to represent a mono-dimensional rough object variations defined as

$$\begin{aligned} \text{rect.}(x) &= 1;\ \ |x| \leq a/2 \\ &= 0 \quad \text{otherwise.} \end{aligned}$$

It is well-known that the autocorrelation of the rectangular function is a triangular function of width $2a$. This reasoning leads us to obtain the cross-sectional dimensions of the grains forming the diffuser object. In case of the rough object, the autocorrelation profiles are extracted from the autocorrelation images making use of eq. (15) and by analogy of the example of rectangular object, we get eq. (18).

3. Experimental recording of speckle pattern

Specimens of aluminum were polished with different abrasive papers to acquire different surface roughness. The arithmetic mean surface roughness R_{a} of aluminum specimens ranging from 2.1 to 4 μm has been studied using the stylus profilometer. Figure 1 shows the experimental set-up used for recording speckle images for different specimens. The rough object is illuminated with a spatially filtered He–Ne

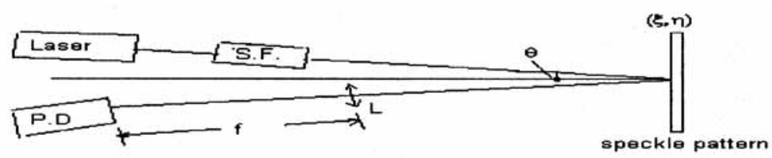

Figure 3. Recording of the autocorrelation function at the plane (x', y') conjugate to the rough object plane $g(x, y)$ from the speckle pattern situated in the plane (ξ, η). SF: spatial filter; L: lens of focal length $f = 15$ cm.

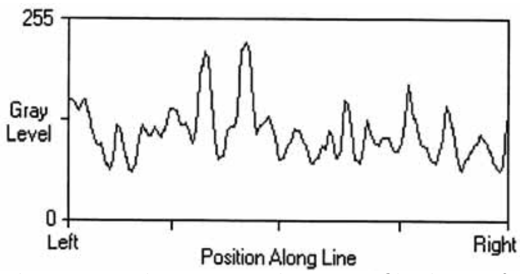

Figure 4. The autocorrelation profile shape of the diffuse object corresponding to a roughness $R_{\mathrm{a}} = 4$ μm.

laser of power 10 mW using a microscope objective lens L_1 followed by a pinhole and then a collimating lens L_2. The scattered coherent wavelets are collected by a CCD camera placed in the focal plane of the Fourier transform lens. The numerical aperture NA of the optical system is kept constant for all the studied surfaces. Figure 2 (left) shows the recorded speckle images for the three different roughnesses at $\lambda = 0.6328$ μm. The measurements are taken at the ambient room temperature 27°C and the chemical processing of the recorded images is done at linear conditions. This will lead to a linear relation between the transmitted complex amplitude and the recorded intensity.

4. Determination of the average surface roughness from the autocorrelation intensity results

High-resolution photographic plates are used to record the speckle pattern. After chemical processing of the photographic plate under linear conditions, the transparency obtained has amplitude proportional to the recorded intensity. The scattered light of this new transparency recorded in the back focal plane of the Fourier transform lens L will represent the autocorrelation function located in the plane (x', y') conjugate to the object plane (x, y) as shown in figure 3. Figure 2 (right) shows the autocorrelation images of the diffuse object recorded at different roughnesses of 2.1 μm, 2.9 μm, and 4 μm. It is common to cite that $R_{\mathrm{a}} = 0$ corresponds to a smooth surface and the selection of the examined surfaces of aluminum is chosen arbitrarily based on polishing the surfaces with abrasive papers.

Figure 4 is showing a gray level profile of the recorded autocorrelation intensity of the diffuse object corresponding to roughness equal to 4 μm. This profile shape is

Table 1. Measured width W of the autocorrelation intensity obtained from the different profile lines at magnification $M = 800$.

	Line 1 (cm)	Line 2 (cm)	Line 3 (cm)	Line 4 (cm)	Line 5 (cm)	Line 6 (cm)
	0.8	0.35	0.9	1.2	0.9	1.2
	0.55	0.8	0.8	0.7	0.6	0.45
	0.8	0.8	0.6	1	1.2	0.75
	0.8	0.55	0.3	0.6	0.55	0.6
	0.45	0.5	0.4	0.9	0.45	0.8
	0.5	0.4	0.4	0.8	0.6	0.7
	0.6	0.85	1.05	0.45	1.55	0.75
	0.5	0.6	0.95	0.7	0.55	0.4
	0.8	0.4	1	0.4	0.7	0.65
	0.5	0.4	0.55	0.55	0.5	0.9
	0.6	0.8	0.7	0.7	0.25	0.65
	0.7	0.5	0.6	0.6		
	0.4	0.6	0.75			
$\langle W \rangle$	0.615	0.581	0.692	0.716	0.714	0.714

obtained from the autocorrelation intensity images recorded in figure 2 (right). The profile line shapes of the autocorrelation intensities are obtained at different heights and it is shown that the shapes are affected by noises. These noises are mainly resulted from the non-uniformity or the irregular distribution of the rough surface. The arithmetic average surface roughness R_a is measured from the autocorrelation function using the relation

$$R_\mathrm{a} = \frac{1}{2M}\langle W \rangle. \tag{18}$$

In eq. (18), $\langle W \rangle$ is the mean width of the autocorrelation intensity due to a series of measurements made at different heights and $M = M_1 \cdot M_2$ is the total magnification where M_1 stands for the optical and $\cdot\ M_2$ stands for the electronic magnification. The factor 2 that appeared in eq. (18) is put in the case of symmetrical rough object, where it is known that width of the autocorrelation function is two times the width of the object. Tables 1–3 show the measured widths W of the autocorrelation intensities obtained from the different profile lines corresponding to different roughnesses.

The total average width of the autocorrelation intensity from the results shown in table 1 is computed as

$$\begin{aligned}\langle W \rangle &= (\Sigma W_i)/N \\ &= (0.615 + 0.581 + 0.692 + 0.716 + 0.714 + 0.714)/6 \\ &= 0.672 \text{ cm},\end{aligned}$$

where W_i is the width of the autocorrelation intensity at the line i and $N = 6$ is the total number of measurements.

Table 2. Measured width W of the autocorrelation intensity obtained from different profile lines at magnification $M = 800$.

	Line 1 (cm)	Line 2 (cm)	Line 3 (cm)	Line 4 (cm)	Line 5 (cm)
	0.45	0.4	0.65	0.15	0.15
	0.3	0.15	0.25	0.35	0.6.1
	0.25	0.6	0.4	0.6	0.2
	0.9	0.3	0.55	0.6	0.45
	0.2	0.3	0.7	0.1	0.4
	0.3	0.7	0.9		0.5
	0.35	0.6	0.9		0.25
	0.7	0.7			0.3
	0.25	0.4			0.8
					0.9
$\langle W \rangle$	0.41	0.46	0.62	0.36	0.4

Table 3. Measured width W of the autocorrelation intensity from the different profile lines and the magnification $M = 800$.

	Line 1 (cm)	Line 2 (cm)	Line 3 (cm)	Line 4 (cm)	Line 5 (cm)
	0.15	0.3	0.4	0.2	0.8
	0.35	0.75	0.2	0.2	0.3
	0.55	0.7	0.15		
	0.6	0.4	0.2		
	0.1	0.3	0.3		
	0.3	0.3	0.2		
	0.25		0.25		
	0.1				
$\langle W \rangle$	0.3	0.45	0.24	0.4	0.55

From eq. (8) the measured mean surface roughness R_{a} is computed as

$$R_{\mathrm{a}} = \frac{1}{2M}\langle W \rangle = 0.762/(1600) = 4.2\ \mu\mathrm{m}.$$

It is shown that the computed value of surface roughness deviates from the result made by the profile meter by only 0.2 μm. The dispersion of the width W_i is due to the randomness of the rough object. Hence, the selection of $N = 6$ corresponds to different arbitrary selection of six different sections and taking the average. Also, the Fourier transformed areas of the speckle images are selected arbitrarily.

Other results of average surface roughness from the profile shapes are obtained at different roughnesses and represented in tables 2 and 3.

The total average width of the autocorrelation intensity obtained from the results shown in table 2 is found to be 0.45 cm. From eq. (18), the measured mean surface roughness R_a is 2.8 μm which deviates from stylus measurement by 0.1 μm.

The total average width of the autocorrelation intensity from the results shown in table 3 is found to be 0.388 cm. From eq. (18) the measured mean surface roughness R_a is 2.36 μm which deviates from the stylus measurement by 0.26 μm.

5. Conclusion

The calculated autocorrelation function of the diffuse object is used to measure the average surface roughness R_a. The measurements are obtained from the computation of widths of the profile shapes of the autocorrelation. The method showed an agreement with the measurements made by the profile meter. This quantitative method is dependent upon the linear imaging using coherent light for the illumination.

References

[1] J W Goodman, Statistical properties of laser speckle patterns, in *Laser Speckle and Related Phenomena* edited by Dainty, Vol. 9. of Topics in Applied Physics (Springer-Verlag, Berlin, 1975) pp. 9–75
[2] M Francon, *Laser speckle and application in optics* (Academic Press, New York, 1979) p. 121
[3] H Fujii and T Asakura, *J. Opt. Soc. Am.* **67**, 1171 (1977)
[4] A M Hamed and M El-shabshiry, *Opt. Applicata* **13**, 317 (1983)
[5] K A O'Donnell, *Appl. Opt.* **32**, 4922 (1993)
[6] Y Balagurunathan and E R Dougherty, *Opt. Eng.* **42**, 1795 (2003)
[7] J M Bennett and L Mattson, Introduction to surface roughness and scattering, Ch. 2–4, pp. 7–55. *Opt. Soc. Am.* Washington DC, 1989
[8] Y Fainman, E Lenz and J Sbamir, *Appl. Opt.* **21**, 3200 (1982)
[9] T Horiuch, Y Tomita and R Hammel, *Jpn. J. Appl. Phys.* **21**, 743 (1982)
[10] J C Stover and S A Serati, *Opt. Eng.* **23**, 406 (1984)
S J Ohtsubo, *J. Opt. Soc. Am.* **A3**, 923 (1986)
[11] J Q Whitly, R P Kusy, M J Mayhew and J E Buckthat, *Opt. Laser Technol.* **19**, 189 (1987)
[12] M Mitsui and O Kizuka, *Opt. Eng.* **27**, 498 (1988)
[13] E Marx and T V Vorburger, *Appl. Opt.* **29**, 3613 (1990)
[14] R Silvennoinen, K E Peiponen, T Asakura, Y Zhang, C Gu, K Ikonen and E J Morley, *Opt. Lasers Eng.* **17**, 103 (1992)
[15] M Sato Kurita, M Sato and K Nakano, *Int. J. Jpn. Soc. Mech. Eng.* **35**, 335 (1992)
[16] P Beckmann, Scattering of light by rough surfaces, in *Progress in optics* edited by E Wolf (North-Holland, Amsterdam, 1967) Vol. 6, pp. 55–69
[17] P Beckmann and A Spizzinchino, *The scattering of electromagnetic waves from rough surfaces* (Artech House, Norwood, Mass., 1987) Ch. 5, pp. 70–98
[18] B J Perick, *Appl. Opt.* **18**, 796 (1979)
[19] C Gorecki, *Opt. Laser Technol.* **21**, 117 (1989)
[20] C Gorecki, *Wear* **137**, 287 (1990)

[21] C Gorecki, *Appl. Opt.* **30**, 4548 (1991)
[22] V M Huynh, S Kurada and W North, *Meas. Sci. Technol.* **2**, 831 (1991)
[23] H Fujii, T Asakura and Y Shindo, *Opt. Commun.* **16**, 68 (1976)
[24] S L Toh, H M Sang and C J Tay, *Opt. Lasers Eng.* **29**, 217 (1998)
[25] Lisa C Leonard and Vincent Toal, *Opt. Lasers Eng.* **30**, 433 (1998)
[26] H Fujii, T Asakura and Y Shindo, *J. Opt. Soc. Am.* **66**, 1217 (1976)
[27] U Persson, *Opt. Lasers Eng.* **17**, 61 (1992)
[28] D Leger, E Mathieu and J C Perrin, *Appl. Opt.* **14**, 872 (1975)
[29] D Leger and J C Perrin, *J. Opt. Soc. Am.* **66**, 1210 (1976)
[30] B Ruffing and J Anschutz, *Proc. Soc. Photo. Opt. Instrum. Eng.* **814**, 105 (1987)
[31] A M Hamed, H El-Ghandoor, F El-Diasty and M Saudy, *Opt. Laser Technol.* **36**, 249 (2004)
[32] Cho Jui Tay and Chenggen Quen, *Optik*, **114**, 1 (2003)
[33] C J Tay, S L Toh, H M Shang and J B Zhang, *Appl. Opt.* **34**, 2324 (1995)
[34] J J Ohtsubo, *Opt. Soc. Am.* **A3**, 982 (1986)
[35] J Whitey, R P Qusy and M J Mayhew, *Opt. Laser Technol.* **19**, 189 (1987)
[36] J D Gaskill, *Linear systems, Fourier transforms, and optics* (John Wiley & Sons, Inc., 1978)